Canadian Science Publishing | Canadian Journal of Forest Research

Unsupervised algorithms to detect single trees in a mixed-species and multi-layered Mediterranean forest using LiDAR data

Journal:	*Canadian Journal of Forest Research*
Manuscript ID	cjfr-2020-0510.R1
Manuscript Type:	Article
Date Submitted by the Author:	10-May-2021

Complete List of Authors:	Alvites, Cesar; Università degli Studi del Molise, Dipartimento di Bioscenza e Territorio Santopuoli, Giovanni; Università degli Studi del Molise, Dipartimento di Agricoltura, Ambienti e Alimenti; Università degli Studi del Molise, Centro di Ricerca per le Aree Interne e gli Appennini (ArIA) Maesano, Mauro; University of Tuscia, Department of Innovation in Biological, Agro-food and Forest Systems Chirici, Gherardo; Universita degli Studi di Firenze Dipartimento di Gestione dei Sistemi Agrari Alimentari e Forestali, Moresi, Federico Valerio; University of Tuscia, Department of Innovation in Biological, Agro-food and Forest Systems Tognetti, Roberto; Università degli Studi del Molise, Dipartimento di Agricoltura, Ambiente e Alimenti; Università degli Studi del Molise, Centro di Ricerca per le Aree Interne e gli Appennini (ArIA) Marchetti, Marco; Università degli Studi del Molise, Dipartimento di Bioscenza e Territorio; Università degli Studi del Molise, Centro di Ricerca per le Aree Interne e gli Appennini (ArIA) Lasserre, Bruno; Università degli Studi del Molise, Dipartimento di Bioscenza e Territorio

Keyword:	Tree detection, Airborne Laser Scanning (ALS), Forest structure, Carbon stock, Climate-Smart Forestry
Is the invited manuscript for consideration in a Special Issue? :	CLIMO 2019

SCHOLARONE™ Manuscripts

Unsupervised algorithms to detect single trees in a mixed-species and multi-layered Mediterranean forest using LiDAR data

Cesar Alvites [*,1], Giovanni Santopuoli [2,3], Mauro Maesano [4], Gherardo Chirici [5], Federico Valerio Moresi [4], Roberto Tognetti [2,3], Marco Marchetti [1,3], Bruno Lasserre [1]

*Corresponding author: Cesar Alvites (cesar.alvites@unimol.it)

1 Dipartimento di Bioscienze e Territorio, Università degli Studi del Molise, Cda Fonte Lappone snc, 86090 Pesche (IS), Italy –(cesar.alvites@unimol.it, marchettimarco@unimol.it, lasserre@unimol.it)

2 Dipartimento di Agricoltura, Ambiente e Alimenti, Università degli Studi del Molise, Via De Sanctis snc, 86100 Campobasso, Italy– (giovanni.santopuoli@unimol.it, tognetti@unimol.it)

3 Centro di Ricerca per le Aree Interne e gli Appennini (ArIA), Università degli Studi del Molise, Via De Sanctis snc, 86100 Campobasso, Italy

4 Department of Innovation in Biological, Agro-food and Forest Systems, University of Tuscia, 01100 Viterbo, Italy; (f.v.moresi@gmail.com; m.maesano@unitus.it)

5 Dipartimento di Scienze e Tecnologie Agrarie, Alimentari, Ambientali e Forestali, Università degli Studi di Firenze, Via San Bonaventura 13, 50145 Firenze, Italy – (gherardo.chirici@unifi.it)

Abstract

Accurate measurement of forest growing stock is a prerequisite for implementing Climate-Smart Forestry strategies. This study deals with the use of Airborne Laser Scanning data to assess carbon stock at the tree level. It aims to demonstrate that the combined use of two unsupervised techniques will improve the accuracy of estimation supporting sustainable forest management. Based on the heterogeneity of tree height and point cloud density, we classified 31 forest stands into four complexity categories. The point cloud of each stand was further splitted in three horizontal layers improving the accuracy of tree detection at tree level for which we calculated volume and carbon stock. The average accuracy of tree detection was 0.48. The accuracy was higher for forest stands with lower tree density and higher frequency of large trees, as well as dense point cloud (0.65). The prediction of carbon stock was higher with a bias ranging from -0.3 % to 1.5 % and the RMSE ranging from 0.14 % to 1.48 %.

Keywords: Tree detection; Airborne Laser Scanning (ALS), Forest structure, Carbon stock, Climate-Smart Forestry.

1. Introduction

In Europe, forests cover about 35 % of the total land area (SoEF 2020) and play a significant role in climate change mitigation thanks to their capacity to remove carbon dioxide from the atmosphere and to store carbon in timber (Nabuurs et al. 2018). Improving the storage of carbon through mitigation techniques and the adaptation of forest ecosystems to climate change, namely managing the forest in a responsible way, supporting the provision of socio-economic and environmental benefits, requires advanced knowledge and continuous update of forest inventory data (Lindner and Karjalainen 2007). However, traditional forest inventory methods are time-consuming and require enormous efforts, particularly in multi-layered forests or poorly accessible forest areas, like those in mountain areas. In these environments, time-efficient and accurate techniques are required to facilitate data acquisition, particularly to provide timely forest management responses facing climate change in threatened forest ecosystems, such as those of Mediterranean mountains. Information about forest area, forest damages, tree species composition, growing stock, and carbon stock is increasingly important to develop climate change mitigation and adaptation strategies for the management of forest ecosystems (Santopuoli et al. 2020b), while maintaining the full set of ecosystem services, in short Climate-Smart Forestry (CSF). Bowditch et al. (2020) ranked sustainable forest management indicators to assess CSF, based on their usefulness to monitor forest adaptation and mitigation. Among others, growing stock and carbon stock, were considered highly important for CSF. In the last decades, several studies focused on the use of remote sensing for assessing forest growing stock and carbon stock (Chirici et al. 2008). Since the early 2000s, the use of Light Detection and Ranging (LiDAR) has considerably increased in the forest sector, particularly the Airborne Laser Scanning (ALS), which is a sensor mounted on aerial vehicles (Næsset 1997). ALS provides advantages in the prediction of forest inventory variables at different scales, from the landscape to the stand levels (Chirici et al., 2016), and even at single tree level for mixed (Mongus and Žalik 2015) and pure stands (Shao et al. 2018). The accuracy of prediction is higher for the individual tree-based approach compared to the area-based approach, as demonstrated for example by Yu et al. (2010). Despite the increased use of ALS devices for assessing forest inventory variables, the individual tree-based approach remains very challenging, particularly for trees belonging to the understory layers of multi-layered and mixed forests (Sačkov et al. 2016).

We propose that ALS may allow quantifying and monitoring smartness indicators in response to rapidly changing environmental conditions, while collecting detailed information on stand productivity, tree health, and species diversity from forest patches. Nevertheless, studies using ALS data to characterize mixed forests showed that the identification of single trees is strongly influenced by forest structure, such as tree species composition, tree height stratification, and stand density (Liang et al. 2019; Wang et al. 2019). Accordingly, better results at single tree level were obtained in regular forest structures, such as pure conifer stands or forest plantations (Dalponte et al.2015; Torresan et al. 2020). Indeed, the individual tree-based approach is difficult to implement in natural and unmanaged forests due to the challenges for deriving single tree-related forest inventory variables e.g. in mature secondary upland and floodplain forests of USA (Duncanson et al. 2014) and in mountain forests of Italian Alps (Kandare et al. 2016) which serve as an important benchmark for CSF.

Recently, many approaches have been developed to exploit ALS point clouds for detecting single trees. Kandare et al. (2014) and Sačkov et al. (2016) used respectively the K-means algorithm and reFLex algorithm, showing several limitations for detecting understory vegetation layers. Both methods detected about 46 % of trees with height lower than 12 m through K-means and 18 % of all trees in intermediate and suppressed layers through reFLex. To improve the detection accuracy, some authors suggested to split the point clouds into several tiles simulating the vertical distribution of trees in the forests, obtaining a higher detection accuracy for trees in the understory layers (68%) (Hamraz et al. 2017). Further approaches, such as RANSAC (RANdom SAmple Consensus) algorithm (Balsi et al.

2018) and MCGC (Multi-Class Graph Cut) (Williams et al. 2019), have been used for tree segmentation with interesting results for trees belonging to large diameter classes (>30 cm), but with uncertain results for trees with a diameter at breast height < 30 cm. In particular, RANSAC algorithm allowed detecting about 86 % of trees in the overstory layer, while MCGC method allowed detecting approximately 30 % of trees in the understory layer. Overall, the accuracy of the detection rate is higher for trees belonging to the top canopy, rather than for those in the understory vegetation. We hypothesize that the combined use of the clustering approach and the stratification of point clouds may improve the accuracy of results, even with low density ALS point clouds. Though trees of understory layer contribute less to the forest carbon sink in comparison with those of the overstory layer, they are crucial for the resilience and the stability of forests, thus contributing to mitigate the effects of climate change (Antos 2009) and ensuring the continuity of forest regeneration and successional processes (Jules et al. 2008).

In particular, describing the vertical structure of multi-layered stands, such as the Mediterranean mountain forests that are characterized by a complex stratification of canopy layers and a mixture of tree species, is a difficult task. Despite their continuous improvement, individual tree-based approaches for delineating vertically heterogeneous canopies remain of difficult application, because of the requirement of site-specific parameters and the geometry of multi-canopy layers (Hamraz et al. 2017). Developing a suitable method for fostering the segmentation of trees in a multi-layered mixed forest through remote sensing techniques is crucial to support CSF, particularly with the objectives of reducing the loss of biodiversity and increasing the adaptation of trees facing climatic changes.

In this study, we combined, for the first time, two unsupervised techniques to identify individual trees in order to assess carbon stock at the tree level in a mixed-species and multi-layered forest, using ALS data. To reach this objective, we firstly focused on the identification of single trees and subsequently showed the changes in the accuracy of detection rate across the three canopy layers. The successful use of these unsupervised techniques in combination might provide a great contribution in monitoring forest ecosystems and collecting CSF indicators.

2. Materials and Methods

2.1. Study area

The study area is located in Central Italy (Molise; 41°42′ N, 14° 12′ E), namely Bosco Pennataro (Figure 1). Bosco Pennataro is recognized as part of the core area of the Collemeluccio-Montedimezzo Alto Molise Man and Biosphere (MaB) Reserve and included in the Natura 2000 network. Bosco Pennataro is a mixed Mediterranean forest with 13 tree species, Turkey oak (*Quercus cerris* L.; 40 %), European beech (*Fagus sylvatica* L.; 21 %), and Italian maple (*Acer obtusatum* Mill.; 9.6 %) being the most frequent ones (Santopuoli et al. 2019). The natural forest community is Aremonio agrimonioidis - Quercetum cerridis (Biondi et al. 2010), classified as Oak-hornbeam according to the European Forest Type (Barbati et al. 2014). The mean altitude of Bosco Pennataro is about 930 m a.s.l., while the average annual precipitation and temperature are 723.5 mm year^{-1} and 14.5 °C, respectively (https://power.larc.nasa.gov). The current management system is high forest with continuous canopy cover and uneven aged mixed species trees. The average stand density is about 700 trees ha^{-1}, the growing stock is 385 m^3 ha^{-1} of which 366 m^3 ha^{-1} are living trees and 19 m^3 ha^{-1} are standing dead trees (Santopuoli et al. 2019).

The absence of forestry interventions over the years has facilitated the conversion from even-aged to uneven-aged forest, supporting the shift of stand structure, from monolayer to multilayer.

The field survey used the one-per-stratum stratified sampling scheme (Barabesi et al. 2012). This sampling strategy partitions a region into several equal-size strata and selects one portion for each stratum based on random and uniform criterion. Based on one-per-stratum scheme, Bosco Pennataro was stratified into 50 strata. One squared plot (hereafter ADS) of 529 m^2 per each stratum was randomly selected and considered for the ALS study. Since the ALS strips covered only partially Bosco Pennataro, we selected the ADS covered by ALS data, and 31 out of 50 ADS were selected (Figure 1).

[FIGURE 1]

2.2. Ground truth data

The forest-related characteristics within each ADS were collected in 2016, using the Field-Map technology (https://www.fieldmap.cz/). The sampled parameters were: tree position, tree crown area, tree species, tree height (TH, m), height of the first branch insertion (I, m), and diameter at breast height (DBH, cm) for all trees with a DBH ≥ 2.5 cm. The stem volume (VOL, m^3) was calculated through allometric equations developed for the Italian tree species (Tabacchi et al. 2011) and used in the National Forest Inventory. The carbon stock stored in stems and large branches with diameter ≥ 5 cm (CS, tons) was calculated by multiplying the aboveground biomass (AGB, tons) by 0.5 (Federici et al. 2008), following the equation (1):

$$AGB = GS * BEF * WBD * A \qquad \text{(eq. 1)}$$

where:

AGB — aboveground biomass, (tons);

GS — growing stock (m^3 ha^{-1});

BEF — biomass expansion factor, which is equal to 1.47;

WBD — wood basal density (t d.m. m^{-3} f.v.), which is equal to 0.38;

A — forest area occupied by a specific forest category (ha^{-1}).

According to Federici et al. (2008), "other broadleaved" forest category was used for BEF and WBD values.

2.3. ALS data collection and analysis

The ALS data were collected in June 2016, in leaf-on forest canopy condition, by Oben s.r.l. company (https://www.oben.it/sito/). The LiDAR sensor (YellowScan Mapper) was mounted on an ultra-light vehicle able to collect 3 echoes per laser pulse, with an average point cloud density equal to 60 points m^{-2} and accuracy equal to ± 15 cm (± 50° of Scan angle and pulse frequency of 20 kHz). However, most of the points belonged to the first echo. The ultra-light vehicle flew at an altitude of 100 m above the ground level.

In this study, a step by step methodological approach was implemented, consisting of the following five steps: 1) pre-processing of the ALS data; 2) grouping and stratifying the ADS point clouds; 3) tree detection and segmentation; 4) validation of the predicted tree crowns; and, 5) prediction of forest inventory variables (Figure 2).

[FIGURE 2]

2.3.1. Step 1 - Pre-processing of ALS data

As part of the preprocessing step, the computing of ALS point cloud was carried out through several modules embedded in LAStools software (www.rapidlasso.com). Initially, the raw ALS point cloud was classified in ground and non-ground strata using the "lasground" module, then, the points marked as outlier were filtered using "lasheight" to generate a point cloud classified and cleaned. The generated point cloud was height normalized, based on ground surface, using "lasheight" module to derive a normalized above-ground point cloud source. The normalized above-ground point cloud was clipped based on the ADS dimension using "lasclip" module. To include the crowns of the edge trees, the areas of ADS were enlarged with a buffer of 2 m, shifting from 529 m^2 to 729 m^2. The enlarged clipped point clouds for each ADS were used as input variables in the following steps.

2.3.2. Step 2 - Grouping and stratifying the ADS point cloud

To investigate factors influencing the accuracy of tree detection, due to the mixed-species and multi-layered characteristics of forest stands, the ADS point clouds were split in four groups (A, B, C, and D) according to the forest stand condition (i.e., tree height variation) and the point clouds density. This step was necessary to classify different complexity levels of the forest stand in more homogeneous groups, according to the sample probability distribution theory (Barabesi et al. 2012). Based on the mean values of both the Average Point Density (APD) (Hamraz et al. 2017, 2017a) and the standard deviation of surveyed tree heights (TH_{sd}) (Liang et al. 2019; Wang et al. 2019a), four groups containing uniform number of observations, i.e., ADS, were discriminated (Figure 3). The value adopted as a threshold for APD was fixed at 31.02 points m^{-2}, while for TH_{sd} the value was established at 6.879 m. Group A included the ADS that showed the lowest values of both APD and TH_{sd}; group B included ADS with lowest values of APD and highest values of TH_{sd}; group C included ADS with highest values of both APD and TH_{sd}; group D included the ADS with highest values of APD and lowest values of TH_{sd}. The grouping process was achieved using “TreeLS" (available on GitHub, https://github.com/tiagodc/TreeLS) and "stats" (authors, R Core Team, and contributors worldwide) R packages.

Moreover, the four groups were ranked in four complexity categories (“highly difficult”, “moderately difficult”, “highly easy”, “moderately easy”) (Liang et al. 2018, 2019; Wang et al. 2019) to discriminate the accuracy of the detection approach within different forest structures (Figure 3).

In details, the ADS characterized by the highest number of trees with a higher frequency of small trees (DBH ≤ 20 cm), as for example ADS of group A and D, were in the categories “highly difficult” and "moderately difficult" respectively, though with differences in the APD values, which were 21.9 points m^{-2} for ADS of "highly difficult" and 106.6 points m^{-2} for ADS of the "moderately difficult". Conversely, the ADS belonging groups B and C, characterized by the lowest number of trees with a higher frequency of large trees (DBH > 20 cm), were in the categories "moderately easy" and "highly easy", respectively, with values of APD equal to 100.3 points m^{-2} for highly easy category and 19.75 points m^{-2} for moderately easy category. Therefore, the ALS and forest stand conditions preserved the structural heterogeneity between ADS, while maintaining the structural homogeneity within categories, which supports the assumption that an appropriate sample probability distribution of ADS was sampled (Barabesi et al. 2012).

[FIGURE 3]

Thereafter, to simulate the vertical stratification of the forest stands, each ADS point cloud was split in three canopy layers, from suppressed to top canopy trees; Layer1 representing the vegetation of the suppressed trees, Layer2 representing the subdominant trees and Layer3 representing the dominant and codominant trees. The splitting procedure based on the vertical distribution of the tree heights, namely 33^{th} (Layer1), 66^{th} (Layer2), and 99^{th} (Layer3) percentiles (Figure 3), was done using "lascanopy" module available on LAStools software. The resulted tiled point clouds were used as input data for the tree detection and segmentation (step 3).

2.3.3. Step 3 - Tree detection and segmentation

To detect the stem position and to segment stem and crown of each single tree, the combined use of Density-Based Spatial Clustering of Applications with Noise (DBSCAN) (Ester et al. 1996) and K-means, was implemented.

DBSCAN is an unsupervised clustering algorithm able to discover the clusters, the noise and the outliers in a database, with poor knowledge of arbitrary shapes. Conceptually, the Density-Based clustering approach is referred to a set of points (p) belonging to a database (D); $p \in D$. The DBSCAN algorithm strives to estimate the quantity of points (p) around each point in a database (D) based on a Euclidean distance measurement called Eps-neighborhood distance. The Eps-neighborhood of each point, named $N_{Eps}(p)$, can be derived following the equation:

$$N_{Eps}(p) = \{q \in D \mid dist(p,q) \leq Eps\} \qquad \text{(eq.2)}$$

Where p and $d \in D$, dist is the distance. In density-based clustering, p is located within the Eps-neighborhood distance. Nevertheless, the size of $N_{Eps}(p)$ around each point relies on a specific minimum number of points used to form a dense region, called MinPts.

$N_{Eps}(p)$ and MinPts are mandatory thresholds to classify the point dispersion into core, border and noise points (Ester et al. 1996; Smits et al. 2012). The core point consists of a high density of points based on MinPts ($N_{Eps}(p) \geq$ MinPts); the border is a point out of the core point but easy to be reachable ($p \in N_{Eps}(q)$); the noise point is an isolated point far away form the core point (Figure 4). To define the core, border and noise points, the DBSCAN algorithm plays an internal validation based on the density-reachability and density-connectivity (Figure 4) (Ester et al. 1996; Smits et al. 2012).

[FIGURE 4]

K-means is an unsupervised clustering algorithm able to partition a database into K clusters for N dimensions, with high intra-class similarities, based on the concept that the K parameter has to be set (Hartigan & Wong 1979). The K-means equation is:

$$j = \sum_{j=1}^{K}\sum_{i=1}^{n} \| X_i^{(j)} - C_j \|^2 \qquad \text{(eq. 3)}$$

Where *j* is the K-means function, *"K"* is the number of clusters, *n* is the number of cases, *X* is a case *j* and *C* is a centroid for cluster *j*.

To retrieve the value of "*K"* cluster from all three canopy layers in order to run the partition of the K-means processing, the DBSCAN was applied for each canopy layer (i.e., Layer1, Layer2 and Layer3) of 31 ADS point clouds.

K-means algorithm allowed us to delineate the tree crown boundary of detected tree positions, using the *"K"* number of clusters derived by DBSCAN findings (Figure 5).

[FIGURE 5]

Since the MinPts and $N_{Eps}(p)$ were pre-requisites to run DBSCAN algorithm, we manually calculated these two values (Ferrara et al. 2018). In particular, the "MinPts" was set to 7 and the "$N_{Eps}(p)$" was set to 0.5 (Figure 5). The analysis was developed in R software, through the "TreeLS" package (available on GitHub, https://github.com/tiagodc/TreeLS), "dbscan" and the "kNNdist" function (Hahsler et al. 2019).

Since the *"K"* number of clusters was provided by DBSCAN processing (Kandare et al. 2016; MacQueen 1967), the number of K-means clusters was the same. Each K-means cluster was composed by the *"K"* centroids (tree position) and *"K"* clusters (tree crown dimension). To remove the noise contained in the predicted tree clusters, we used Mahalanobis distance using R packages "TreeLS", "akmeans" (Kwak 2014), "rgdal" (Bivand and Rowlingson 2016) and "rLiDAR" (Silva et al. 2015). ALS metrics were extracted for each truly detected tree through the "lascanopy" module implemented in LAStools software. The point cloud data for each potential stem were exported and validated in the following step.

2.3.4. Step 4 - Validation of predicted tree crowns

The validation accuracy of the DBSCAN and K-means results was carried out following the most commonly used accuracy parameters in ALS detection studies (Sačkov et al. 2016). More precisely, the accuracy of the tree position and tree crown delineation was achieved by comparing the reference data (tree position, tree crown dimension from field survey) with the predicted data (centroid of stems, tree crowns from ALS data) through the Euclidean distance, with a tolerance value of three meters, as reference values to validate the detection accuracy. Specific accuracy parameters were:

- True-positive (TruePos; units), representing the correctly identified tree.
- False-positive (FalsePos; units) was the commission error, representing the trees that could not be associated to any surveyed tree (i.e., identified but not real).
- False-negative (FalseNeg; units) was the omission error, representing the non-segmented tree.
- Percent tree crown overlap (TREE CROWN OVERLAP; %), as the parameter indicating the difference between the isolated reference and predicted crown segment.
- Distance between the predicted centroid of the crown segment and the centroid of the reference crown (Euclidean distance; m). Euclidean distance was applied to determine the distance between the predicted and reference centroid crown segments.
- Detection Rate (DR; %), reporting the relationship between the TruePos and the reference stem.
- Time for tree detection (Time for TD; sec), reporting the time consuming in analyzing each ADS of 729 m^2 using a personal compute Inter® Core™ i7-7500U CPU, 2.70 GHz and 8,00 GB RAM.

2.3.5. Step 5 - Prediction of forest inventory variables

To predict different forest inventory variables, for trees that were previously identified, the Random Forests algorithm was applied. Random Forests algorithm allowed us to achieve regression tree classification based on decision trees (Breiman 2001), as being widely used to handle a high number of factors and for reducing the overfitting (Shi et al. 2018).

The Random Forests parameters used for the prediction were (a) “Ntree”, the number of decision trees to be used during the prediction phase; (b) “Mtry”, the number of input variables for splitting at each tree nodes; and (c) “nodesize”, the minimum size of terminal nodes (Belgiu and Drăgu 2016).

In this study, the three forest inventory variables (i.e., DBH, TH, and VOL) for each layer (i.e., Layer1, Layer2 and Layer3, and Layer1-Layer3) within each category (i.e., highly difficult, moderately difficult, highly easy, moderately easy) were predicted using the ALS metrics (Top-nine) of its corresponding TruePos. The whole predicted models amount to 48: 16 out of 48 corresponding to DBH, 16 out of 48 corresponding to TH and 16 out of 48 corresponding to VOL. Furthermore, to investigate the performance of models using the ALS metrics (Top-nine) given to the total TruePos, we calculated the forest inventory variables (i.e., DBH, TH, and VOL) using the merged information of categories; the whole predicted models were three, one per forest inventory variable.

The Random Forests models were implemented using the randomForest package in R (Liaw and Wiener 2002). The setting of the Random Forests algorithm was implemented by "Ntree" as 1000, "Mtry" as 3-4, and node size as 5. The validation of these models was developed by the coefficient of determination (R-squared; 0-1) and root mean square error (RMSE; cm, m, m^3) for the number of trees examined (N°trees; units), using the “stats” (authors, R Core Team and contributors worldwide) and “usdm” (Naimi 2017) R packages.

Moreover, the CS was predicted using as input the VOL from ALS data for each canopy layer. Validation was done by comparing the predicted vs. observed CS amount for each ADS.

3. Results

Bosco Pennataro is characterized by a heterogeneous forest structure; among the ADS, the number of trees ranged between 453 and 3698 trees ha^{-1}, the mean DBH ranged between 9.9 cm and 26.9 cm, the mean TH ranged between 8.2 m and 23.1 m, and the stem volume ranged from 183 m^3 ha^{-1} (carbon amount = 51.1 tons ha^{-1}) to 633.9 m^3 ha^{-1} (carbon amount = 177 tons ha^{-1}). The heterogeneity of the forest stand, due to both vertical stratification and DBH variability, as well as the stand density, impacted on the point density and spacing of ALS point clouds that varied from 12.13 points m^{-2} to 292.9 points m^{-2} (Table 1).

3.1. ADS groups and ALS point cloud layers

The clusterization of the surveyed ADS in four distinct groups allowed us to assess forest inventory variables in this mixed-species and multilayered Mediterranean forest correctly. Though the number of ADS for each group was similar (Figure 6), ADS showed a varying pattern across the complex forest structure (Table 1). Stand density was high in ADS of difficult categories, ranged between 1724 trees ha^{-1} and 1542 trees ha^{-1}. Moreover, these ADS presented high standard deviation values (985 trees ha^{-1} and 840 trees ha^{-1}), compared to those of easy categories (between 339 trees ha^{-1} and 262 trees ha^{-1}). Additionally, the easy categories were characterized by a great number of big trees compared to the difficult categories and, as a consequence, by high values of assessed forest inventory variables, i.e., DBH, TH, VOL, and CS.

[FIGURE 6]

Results showed a greater variability among ADS of the difficult categories rather than among ADS of the easy categories, allowing us to state that the heterogeneity of forest structure impacted on the detection of single trees.

[TABLE 1]

The number of trees across the three canopy layers was rather similar, from Layer1 to Layer3, with a relative low presence of trees in the Layer2 (Figure 7). Therefore, the discrimination of trees was similar also across different ADS.

However, the distinction of crowns across the three canopy layers was facilitated in ADS of easy compared to difficult categories. For this reason, the poor presence of trees, more accentuated in ADS of the “slightly easy” and “moderately easy” categories, was a contributing factor that enabled the discrimination of single trees (Figure 7 B-C); while the high values of stand density created an overlapping effect among tree crowns, which slightly hindered the detection of trees, particularly for the intermediate layers. (Figure 7 A-D).

[FIGURE 7]

3.2. Tree detection

We detected 952 out of 2117 reference trees, reaching an average detection rate of 48 % (Table 2), with a moderate uniformity/similarity across the three layers (SD = ± 12.5). Our tree detection approach was more sensitive to the omission error, 1165 out of 2117 reference trees, than to the commission error, 795 out of 2117 reference trees. Better results in terms of the detection rate were obtained in A belonging to the ADS of groups B and C (easy categories) rather than in those of groups A and D (difficult categories). The detection rate was 36 % (SD = ± 7.3) for ADS of the “highly difficult” category, identifying 261 out of 730 trees. The detection rate was 49 % (SD = ± 19.2) for ADS of “moderately difficult” category, identifying 215 out of 435 trees. The detection rate for ADS of “moderately easy” category was 43 % (SD = ± 7.8), identifying 282 out of 654 trees. The detection rate for ADS of “highly easy” category reached 65 % (SD = ± 7.0), identifying 194 out of 298 trees.

The detection rate values were more accurate for trees of the Layer2 (54 %, SD = ± 13.7) than for trees of the Layer1 (42 %, SD = ± 7.8) and Layer3 (49 %, SD = ± 15.4).

The detection of trees in ADS with the lowest point density, corresponding to the “highly difficult” and “moderately easy” categories, was affected by the occlusion effects from subdominant, codominant and dominant to suppressed tree crowns; a better performance was obtained for trees of the Layer2 and Layer3. Whereas, an opposite pattern was observed in ADS with a higher point density, “highly easy” and “moderately difficult” categories. Hence, the point density influenced the occlusion effects from large to small tree crown dimension in tree detection, regardless the forest structure.

The highest value of the commission error was found for the ADS of the “highly easy” category, which was 123 %, (367 FalsePos), while ranging between 21 % and 25 % in the remaining three categories

Similarly, the highest value of the omission error was found in the “highly easy” category, which was 135 %, (104 FalseNeg), while the omission error for the other three categories ranged between 51 % and 64 %. The best and worst compromise between commission and omission errors were found in ADS of “moderately easy” (106 and 220 out of 435 stems surveyed) and “highly easy” (367 and 104 out of 298 stems surveyed), respectively.

The sensitivity variation of our algorithm for commission and omission errors was rather small among the three canopy layers, ranging from 44 % to 58 % for FalsePos and from 46 % to 58 % for FalseNeg.

[TABLE 2]

The estimation of the crown position displayed similar values for all four categories, ranging between 1.73 m and 2.55 m (Figure 8II). The similarities were also observed among the three canopy layers, particularly for ADS of the “highly easy” category, within which the most homogeneous values were observed. On the contrary, small differences were observed between Layer3 and Layer1 or Layer2 in the remaining categories. Although the observed crown dimension was not completely covered by the predicted tree crown dimension, the average overlap value was 57 %; this was moderately consistent amongst ADS (SD = ± 11) (Figure 8III), within which the Layer2 was the most accurate.

Time required in detecting the trees, using combined unsupervised algorithms, was faster in the ADS with lowest (ranged between 19.7 and 21.9 points m^{-2}) point density in comparison with those with the highest (ranged between 100.3 and 106.6 points m^{-2}) (Figure 8IV).

[FIGURE 8]

3.3. Forest inventory variables

Comparing the predicted vs. observed data from correctly detected trees, corresponding to 952 trees, we found significant values of the coefficient of determination and the RMSE for DBH (0.92; 4.03 cm), TH (0.95; 1.33 m) and VOL (0.82; 0.31 m^3), respectively (Figure 9).

[FIGURE 9]

Despite the different quantity of trees analyzed (TruePos), slight differences in terms of coefficient of determination between predicted vs. observed across categories were observed (Table 3). However, the categories were less accurate for DBH (N°trees = 261 and 215; R-squared = 0.9) belonging to ADS of the “highly difficult” and “moderately easy” categories; whereas, for TH (N°trees = 215; R-squared = 0.93) and VOL (N°trees = 215; R-squared = 0.89), this was the case for the ADS belonging to the “moderately easy” category. Therefore, the categories with smaller point density (in absolute terms) were slightly less accurate.

[TABLE 3]

We observed that the best and worst accuracies were found in the ADS of the “moderately easy” and “highly difficult” categories, based on the fitted prediction for stem volume (RMSE = 0.14 % and bias

= 0.1 %) and carbon stock (RMSE = 1.48 % and bias = 1.5 %) variables (Table 4). However, we note that the "moderately difficult" category offered better performances than the "highly easy" category. Therefore, ADS with higher number of trees with a higher frequency of small trees were less affected by the performance of the models in terms of bias and RMSE values. Moreover, the bias and RMSE in the case of "moderately easy" and "moderately difficult" categories suggested that the ADS with a higher point densities associated and higher share of trees with the predominance of large trees might solve issues associated with uncertainties. It is worth noting that the prediction of stem volume was weakly related to the tree detection accuracy.

[TABLE 4]

4. Discussion

4.1. Tree detection

Results revealed that the joint use of DBSCAN and K-means allowed detecting nearly half of the trees identified through ALS data in the studied multi-layered and mixed-species Mediterranean mountain forest. Enhanced detection accuracy was obtained in forest stands with higher heterogeneity of tree height, regardless of stand density. This approach may improve monitoring of forest dynamics related to tree growth and surveying of tree mortality due to forest disturbance. Indeed, mixed-species and multi-layered forests in Mediterranean mountains are complex systems and the assessment of their 3D full structure is of importance for reducing uncertainties in the collection of reference data. In particular, consistent ALS monitoring of forest changes may allow deriving new indicators of CSF related to vertical and horizontal forest attributes (Bodwitch et al. 2020; Santopuoli et al. 2020b).

Though the detection was challenging for trees of the understory layer, results obtained here were somewhat encouraging in comparison with those reported by other authors (Table 2). For example, Sačkov et al. (2016) showed accuracy values from 24 % (all trees) to 36 % (trees higher than 16 m) and 48 % (trees higher than 21 m). Similarly, Duncanson et al. (2014) reported values from 21 % for suppressed trees to 70 % for dominant trees, and Hamraz et al. (2017) observed that the accuracy of tree detection decreased from dominant to suppressed trees and highlighted that a dense point clouds was required for a satisfactory detection. The LiDAR point clouds used here had an average of 60 points m^{-2}, ranging between 21 to 106 points m^{-2}. Nevertheless, the choice to split the point clouds into three layers allowed us to improve the overall detection accuracy, supporting the use of ALS data for monitoring forest inventory variables and smart forestry indicators at a large scale. This aspect is crucial to support forest managers with a monitoring tool for well-timed and spatial-explicit forest inventory data, and appears promising for implementing smart management strategies to reduce operating costs (Torresan et al. 2021).

Our study revealed that the point density (Hamraz et al. 2017), the forest stand conditions e.g. stand density (Kandare et al. 2016) and DBH classes (Williams 2019), and the site-specific parameters, e.g., tree species composition (Liang et al. 2019) and forest structure (Sackov et al. 2016) impacted the identification of trees, as well as the detection rate, and commission and omission errors. As a consequence, the density of ALS point clouds would represent one important limitation of unsupervised techniques for detecting single trees, which failed for values below the threshold of 30 points m^{-2}. In particular, the detection accuracy was further worsened in ADS of this Mediterranean mountain mixed-species and multi-layered forest with high values of stand density (1542 trees ha^{-1}).

Beyond the stand density, the presence of large trees was advantageous in the identification processes using our unsupervised approach. Therefore, the detection was more accurate for those ADS with higher average values of DBH and TH, namely veteran trees (Santopuoli et al. 2020a).

It is important to note that, though the detection accuracy was higher for trees belonging to Layer2 and Layer3, a better compromise between omission and commission errors was found in the Layer1 (Table 2). This apparent contradiction was probably related to the higher stand density inducing commission errors but avoiding omission errors, due to the clustering approach and the Mahalanobis filtering of outlier. Dense forest stands may hinder the correct separation between nearby trees (Dalponte et al. 2015). This means that the ALS point density and the forest structure may play a complementary role in identifying and segmenting trees using point cloud sources for multi-layered as well as for two-layered mixed-species forests (Torresan et al. 2020).

The detection performance was improved by the evaluation of the crown radius, which allowed us to obtain good results (ranging between 1.73 m and 2.55 m), somehow better than those reported in the literature. For example, 2 m was the value reported by Shao et al. (2018), 2.5 m by Balsi et al. (2018), 3.5 m by Mongus and Žalik (2015), and 5 m by Sačkov et al. (2016). Contrary to what revealed by these authors, for which the values of Euclidean distance decreased from Layer3 to Layer1, we demonstrated that the detection accuracy could be relatively constant across the three canopy layers. Tree crown overlap ranged between 47.26 % and 82.51 % (more stable values were obtained in ADS of the “highly easy” and “highly difficult” categories), supporting the hypothesis that an optimum performance for identifying and segmenting trees could be expected for multi-layered mixed-species forests of this type.

4.2. Forest inventory variables

The approach implemented in this study allowed us to predict three forest inventory variables, namely DBH, TH, and VOL, reaching the accuracy in coefficient of determination of about 0.92 for DBH, 0.95 for TH, and 0.82 for VOL (Figure 9). Though the feasibility in the prediction approach was tested in four complexity levels, there were not substantial differences in the prediction accuracy among them. Such a versatility of the Random Forests approach increased the prediction performance of forest inventory variables and was proved promising for collecting CSF indicators. It is worth noting that subdividing the ALS data in three canopy layers might describe thoroughly the forest inventory variables for trees within each canopy layer, especially for trees of Layer2 and Layer1.

The performance of VOL models was more accurate using the information of whole TruePos (Layer1-Layer3) compared to the TruePos of the Layer3, based on the RMSE measurements found in all four categories (Table 3). More accurate prediction of DBH and VOL was observed in the "highly difficult" category, whereas, for TH the fitted prediction was observed in all four categories. The effect of the quantity of TruePos on the performance of models was mitigated by the bootstrap approach of the Random Forests algorithm, as supported by almost all RMSE values across the three canopy layers.

As expected, the performance of models based on RMSE values declined from Layer1 to Layer3 for DBH and VOL; however, this pattern was moderately smoothed for TH. This means that the estimation of DBH and VOL for intermediate and dominant trees was a challenging tasks, when the stratification approach was applied; whereas, the prediction for TH was rather accurate for all three canopy layers.

Here, the stand structural heterogeneity and the ALS point density represented the most hindering factors for the prediction, though results were satisfactory and higher than those reported in similar studies. Indeed, the accuracy obtained for the prediction of DBH in this study was higher than in Sačkov et al. (2016, 2019), who reported R-squared equal to 0.71 for mixed-species forest stands, and

0.78 for deciduous and 0.72 for coniferous forests. Yet, for the prediction of VOL, other studies reported lower values of accuracy (Alberti et al. 2013; Sačkov et al. 2016).

The prediction accuracy for carbon stock was more accurate in the ADS with high ALS point density ("moderately difficult"; bias = -0.3 %) and low ALS point density ("moderately easy"; bias = 0.1 %), but with more homogeneous forest structure. Therefore, in the prediction of forest inventory variables, a low ALS density would represent an issue in areas with relatively homogeneous forest structure. Results obtained for the stem volume (where input data to derive the carbon stock was ranged between 0.89 and 0.90 of R-squared) were in line with those observed by other authors: Popescu (2007) showed higher R-squared values for above ground biomass in mature stands of loblolly pine, ranging between 0.88 and 0.93, whereas Allouis et al. (2012) reported higher R-squared values of above ground biomass in individual black pine trees, ranging between 0.87 and 0.91.

Accurate predictions of carbon stock could be expected in all the four categories considered here. However, the bias in prediction (minimum bias = -0.3 % and maximum bias = 1.5 %) could be associated with other factors, e.g., understory vegetation, standing deadwood, terrain slope, site aspect, and tree species richness (White et al. 2014).

Overall, the accuracy of tree detection and carbon stock assessment resulted to be more sensitive to point density than to heterogeneity of forest structure (Table 2; Table 4). This means that further efforts focused on improving the quality of points will be beneficial for better exploiting the potential of tested algorithms. In particular, we found many weakness aspects during the ALS processing. For example, the ADS point clouds characterized by lower, altered and irregularly-spaced densities were hard to process by DBSCAN algorithm; fixed values of minPts and Eps-neighborhood became disadvantageous for identifying the trees in ADS from difficult categories; analyzing the ADS with dense point clouds are time consuming. These weakness aspects suggested that DBSCAN algorithm was sensitive to quality of point cloud and fixed minPts and Eps-neighborhood values (Ahmad and Dang, 2015).

Nevertheless, careful consideration in operational activities could be beneficial to overcome part of these issues, especially before the collection phase: 1) forest canopy structure (changing from leaf-on to leaf-off) (Shao et al 2018); 2) flight strips (changing from 0 % to more than 50 % of overlapped flight strips) (Liang et al 2019) and 3) ALS sensor (changing from 3 echoes to 4-15 echoes) (Kandare et al 2016; Hamraz et al 2017). Since our ultra-light vehicle flew at an altitude of 100 m above the ground level, we hypothesized this flying height was good enough. In conclusion, the quality of the point cloud may vary depending on the ALS sensor returns, operational aspect and forest structure, therefore, the potential of our algorithm can also be affected.

5. Conclusion

This study aimed to improve the use of ALS data for the prediction of forest inventory variables in mixed-species and multi-layered forests of Mediterranean mountain environments. Such a development might represent an important advance for the estimation of forest characteristics and the collection of CSF indicators, as well as to monitor the dynamics of these complex forest ecosystems over time.

The most important limitation faced in this study was the ALS point density. Using very low point density, the detection of single trees was challenging, as for those stands with less than 30 points m^{-2}. ADS primarily composed of big trees would be less problematic. In this latter case, we obtained more than 65 % of detection accuracy, regardless of the canopy layers. Nevertheless, to detect trees in forest areas where small trees are abundant, a denser point cloud would be required. The stratification approach adopted in this study, minimized the negative impacts due to the low point density and the heterogeneity of forest structure, stressing the usefulness of ALS data for assessing forest inventory variables and climate-smart forestry indicators.

However, the heterogeneity of forest structure could be an important hindering factor when using ALS in the understory layer, especially in forest areas with poor ALS densities (>30 points m^{-2}). The occlusion effect of ALS point in tree detection could be caused by highly overlapped crowns, hindering the detection of trees. It is worth noting that the unsupervised technique implemented in this study allowed us to obtain satisfactory accuracy for a forest ecosystem characterized by heterogeneous canopy profile and big tree size.

The application of unsupervised algorithms for detecting single trees in a mixed-species and multi-layered Mediterranean forest through LiDAR data was proved feasible in support of actively measuring and monitoring of complex mountain forest ecosystems. The stratification of ALS point clouds might represent a valid alternative to simulate the vertical distribution of trees in stands with heterogeneous structure, allowing forest operators to detect and monitor a large amount of trees.

Acknowledgments

The study was supported by the FRESh LIFE project “Demonstrating Remote Sensing integration in sustainable forest management” (LIFE14/ IT000414). We wish to thanks Markus Hollaus for its feedbacks aimed at improving the quality of the manuscript. This study was finalized in the frame of the COST (European Cooperation in Science and Technology) Action CLIMO (Climate-Smart Forestry in Mountain Regions - CA15226) financially supported by the EU Framework Programme for Research and Innovation HORIZON 2020.

References

Ahmad, P. H., and Dang, S. 2015. Performance evaluation of clustering algorithm using different datasets. International Journal of Advance Research in Computer Science and Management Studies. 8. 167-173. Available from www.ijarcsms.com [accessed 28 March 2021].

Allouis, T., Durrieu, S., Véga, C., and Couteron, P. 2012. Stem volume and above-ground biomass estimation of individual pine trees from LiDAR data: Contribution of full-waveform signals. IEEE Journal of Selected Topics in Applied Earth Observations and Remote Sensing. 6(2): 924-934. doi.org/10.1109/JSTARS.2012.2211863.

Antos, J. 2009. Understory plants in temperate forests. Forests And Forest Plants, Department of Biology, University of Victoria, Canada. pp. 262-279.

Alberti, G., Boscutti, F., Pirotti, F., Bertacco, C., De Simon, G., Sigura, M., Cazorzi, F., and Bonfanti, P. 2013. A LiDAR-based approach for a multi-purpose characterization of Alpine forests: an Italian case study. iForest biogeosciences and forestry. 6(3): 156. doi: 10.3832/ifor0876-006.

Balsi, M., Esposito, S., Fallavollita, P., and Nardinocchi, C. 2018. Single-tree detection in high-density LiDAR data from UAV-based survey. European Journal of Remote Sensing. 51(1): 679-692. doi.org/10.1080/22797254.2018.1474722.

Barabesi, L., Franceschi, S., and Marcheselli, M. 2012. Properties of design-based estimation under stratified spatial sampling with application to canopy coverage estimation. Annals of Applied Statistics. 6(1): 210-228. doi.org/10.1214/11-AOAS509

Barbati, A., Marchetti, M., Chirici, G., and Corona, P. 2014. European Forest Types and Forest Europe SFM indicators: Tools for monitoring progress on forest biodiversity conservation. Forest Ecology and Management. 321. https://doi.org/10.1016/j.foreco.2013.07.004.

Belgiu, M., and Drăguţ, L. 2016. Random forest in remote sensing: A review of applications and future directions. ISPRS Journal of Photogrammetry and Remote Sensing. 114: 24-31. doi.org/10.1016/j.isprsjprs.2016.01.011.

Biondi, E., Blasi, C., Burrascano, S., Casavecchia, S., Copiz, R., Del Vico, E., Galdenzi, V., Gigante, D., Lasen, C., Spampinato, G., Venanzoni, R. and Zivkovic, L. 2010. Manuale italiano di interpretazione de- gli habitat (Direttiva 92/43/CEE). [Italian guide- lines for habitat interpretation (Directive 92/ 43/CEE)]. MATTM. pp. 20. Available from http://vnr.unipg.it/habitat/ [accessed 15 March 2021].

Bivand, R., and Rowlingson, B. 2016. Package 'rgdal'. R Package. Available from https://cran.r-project.org/web/packages/rgdal/index.html [accessed 15 January 2019].

Bowditch, E., Santopuoli, G., Binder, F., del Río, M., La Porta, N., Kluvankova, T., Lesinski, J., Motta, R., Pach, M., Panzacchi, P., Pretzsch, H., Temperli, C., Tonon, G., Smith, M., Velikova, V., Weatherall, A., and Tognetti, R. 2020. What is Climate-Smart Forestry? A definition from a multinational collaborative process focused on mountain regions of Europe. Ecosystem Services. 43(1):1-13. doi.org/10.1016/j.ecoser.2020.101113.

Breiman, L. 2001. Random forests. Machine learning. University of California Berkeley. pp. 5-32.

Chirici, G., Barbati, A., Corona, P., Marchetti, M., Travaglini, D., Maselli, F., and Bertini, R. 2008. Non-parametric and parametric methods using satellite images for estimating growing stock volume in alpine and Mediterranean forest ecosystems. Remote sensing of Environment. 112(5): 2686-2700. doi:10.1016/j.rse.2008.01.002.

Chirici, G., McRoberts, R.E., Fattorini, L., Mura, M. and Marchetti, M. 2016. Comparing echo-based and canopy height model-based metrics for enhancing estimation of forest aboveground biomass in a model-assisted framework. Remote sensing of Environment. 174. https://doi.org/10.1016/j.rse.2015.11.010

Dalponte, M., Reyes, F., Kandare, K., and Gianelle, D. 2015. Delineation of Individual Tree Crowns from ALS and Hyperspectral data: a comparison among four methods. European Journal of Remote Sensing. 48(1): 365-382. DOI: 10.5721/EuJRS20154821.

Duncanson, L.I., Cook, B.D., Hurtt, G.C., and Dubayah, R.O. 2014. An efficient, multi-layered crown delineation algorithm for mapping individual tree structure across multiple ecosystems. Remote Sensing of Environment. 154: 378-386. doi.org/10.1016/j.rse.2013.07.044.

Ester, M., Kriegel, H.P., Sander, J., and Xu, X. 1996. A density-based algorithm for discovering clusters in large spatial databases with noise. KDD-96 Proceedings. 96(34): 226-231. doi.org/10.1016/B978-044452701-1.00067-3.

Federici, S., Vitullo, M., Tulipano, S., De Lauretis, R., and Seufert, G. 2008. An approach to estimate carbon stocks change in forest carbon pools under the UNFCCC: the Italian case. iForest biogeosciences and forestry. 1(2): 86-95. https://doi.org/10.3832/ifor0457-0010086.

Ferrara, R., Virdis, S.G., Ventura, A., Ghisu, T., Duce, P., and Pellizzaro, G. 2018. An automated approach for wood-leaf separation from terrestrial LIDAR point clouds using the density based clustering algorithm DBSCAN. Agricultural and Forest Meteorology. 262: 434-444. doi.org/10.1016/j.agrformet.2018.04.008.

Hahsler, M., Piekenbrock, M., and Doran, D. 2019. dbscan: Fast density-based clustering with r. Journal of Statistical Software. 91(1): 1-30. DOI: 10.18637/jss.v091.i01.

Hamraz, H., Contreras, M.A., and Zhang, J. 2017. Vertical stratification of forest canopy for segmentation of understory trees within small-footprint airborne LiDAR point clouds. ISPRS Journal of Photogrammetry and Remote Sensing. 130: 385-392. doi.org/10.1016/j.isprsjprs.2017.07.001.

Hamraz, H., Contreras, M.A., and Zhang, J., 2017a. Forest understory trees can be segmented accurately using sufficiently dense airborne laser scanning point clouds. Scientific reports. 7(1): 1-9. DOI: 10.1038/s41598-017-07200-0.

Hartigan, J. A., and Wong, M. A. 1979. Algorithm AS 136: A k-means clustering algorithm. Journal of the royal statistical society. series c (applied statistics). 28(1): 100-108.

Jules, M.J., Sawyer, J.O., and Jules, E.S. 2008. Assessing the relationships between stand development and understory vegetation using a 420-year chronosequence. For. Ecol. Manage. 255(7): 2384-2393. https://doi.org/10.1016/j.foreco.2007.12.042.

Kandare, K., Dalponte, M., Gianelle, D., and Chan, J.C. W. 2014. A new procedure for identifying single trees in understory layer using discrete LiDAR data. In 2014 IEEE Geoscience and Remote Sensing Symposium. 1357-1360. doi.org/10.1109/IGARSS.2014.6946686.

Kandare, K., Ørka, H.O., Chan, J.C.W., and Dalponte, M. 2016. Effects of forest structure and airborne laser scanning point cloud density on 3D delineation of individual tree crowns European Journal of Remote Sensing. 49(1): 337-359. doi: 10.5721/EuJRS20164919.

Kwak, J. 2014. Akmeans: Adaptive K-Means Algorithm Based on Threshold. R package version 1.1. Available from https://CRAN.R-project.org/package¼akmeans. [accessed 15 October 2019].

Liang, X., Hyyppä, J., Kaartinen, H., Lehtomäki, M., Pyörälä, J., Pfeifer, N., Holopainen, M., Brolly, G., Francesco, P., Hackenberg, J., Huang, H., Jo, H-W., Katoh, M., Liu, L., Mokros, M., Morel, J., Olofsson, K., Poveda-Lopez, J., Trocha, J., Wang, D., Wang, J., Xi, Z., Yang, B., Zheng, G., Kankare, V., Luoma, V., Yu, X., Chen, L., Vastaranta, M., Saarinen, N., Wang, Y. 2018. International benchmarking of terrestrial laser scanning approaches for forest inventories. ISPRS journal of photogrammetry and remote sensing. 144: 137-179. https://doi.org/10.1016/j.isprsjprs.2018.11.008.

Liang, X., Wang, Y., Pyörälä, J., Lehtomäki, M., Yu, X., Kaartinen, H., Kukko, A., Eija, H., Issaoui, A.E.I., Nevalainen, O., Vaaja, M., Virtanen, J-P., Katoh, M., and Deng, S. 2019. Forest in situ observations using unmanned aerial vehicle as an alternative of terrestrial measurements. Forest Ecosystems. 6(1): 1-16. DOI: 10.1186/s40663-019-0173-3.

Liaw, A., and Wiener, M. 2002. Classification and regression by randomForest. R news. 2(3): 18-22. Available from https://cran.r-project.org/web/packages/randomForest/randomForest.pdf [accessed 18 October 2020].

Lindner, M., and Karjalainen, T. 2007. Carbon inventory methods and carbon mitigation potentials of forests in Europe: a short review of recent progress. Eur. J. For. Res. 126(2): 149-156. https://doi.org/10.1007/s10342-006-0161-3.

MacQueen, J. 1967. Some methods for classification and analysis of multivariate observations. In Proceedings of the fifth Berkeley symposium on mathematical statistics and probability. University of California Press Berkeley. pp. 281-297.

Mongus, D., and Žalik, B. 2015. An efficient approach to 3D single tree-crown delineation in LiDAR data. ISPRS Journal of Photogrammetry and Remote Sensing. 108: 219-233. doi.org/10.1016/j.isprsjprs.2015.08.004.

Nabuurs, G.J., Verkerk, P.J., Schelhaas, M., González-Olabarria, J.R., Trasobares, A., and Cienciala, E. 2018. Climate-Smart Forestry: mitigation impact in three European regions. From Science to Policy 6. European Forest Institute. pp. 1-32.

Naimi, B. 2017. R package usdm: Uncertainty analysis for species distri- bution models. Available from https://cran.r-project.org/web/packa ges/usdm/usdm.pdf [accessed 18 October 2020].

Næsset, E. 1997. Determination of mean tree height of forest stands using airborne laser scanner data. ISPRS Journal of Photogrammetry and Remote Sensing. 52(2): 49-56. doi.org/10.1016/S0924-2716(97)83000-6.

Popescu, S.C. 2007. Estimating biomass of individual pine trees using airborne lidar. Biomass Bioenergy. 31(9): 646-655. https://doi.org/10.1016/j.biombioe.2007.06.022.

Sačkov, I., Santopuoli, G., Bucha, T., Lasserre, B., and Marchetti, M. 2016. Forest inventory attribute prediction using lightweight aerial scanner data in a selected type of multilayered deciduous forest. Forests. 7(12): 307. doi.org/10.3390/f7120307.

Sačkov, I., Kulla, L., and Bucha, T. 2019. A Comparison of Two Tree Detection Methods for Estimation of Forest Stand and Ecological Variables from Airborne LiDAR Data in Central European Forests. Remote Sens. 11(12): 1431. doi.org/10.3390/rs11121431.

Santopuoli, G., di Cristofaro, M., Kraus, D., Schuck, A., Lasserre, B., and Marchetti, M. 2019. Biodiversity conservation and wood production in a Natura 2000 Mediterranean forest. A trade-off evaluation focused on the occurrence of microhabitats. iForest biogeosciences and forestry. 12(1): 76. DOI: 10.3832/ifor2617-011.

Santopuoli, G., Di Febbraro, M., Maesano, M., Balsi, M., Marchetti, M., Lasserre, B. 2020a. Machine Learning Algorithms to Predict Tree-Related Microhabitats using Airborne Laser Scanning. Remote Sens. 12: 2142. doi:10.3390/rs12132142.

Santopuoli G., Temperli C., Alberdi I., Barbeito I., Bosela M., Bottero A., Klopčič M., Lesinski J., Panzacchi P.,Tognetti R. 2020b. Pan-European Sustainable Forest Management indicators for assessing Climate-Smart Forestry in Europe. Canadian Journal of Forest Research. doi.org/10.1139/cjfr-2020-0166.

Shao, G., Shao, G., and Fei, S. 2018. Delineation of individual deciduous trees in plantations with low-density LiDAR data. International journal of remote sensing. 40(1): 346-363. doi.org/10.1080/01431161.2018.1513664.

Shi, Y., Wang, T., Skidmore, A.K., and Heurich, M. 2018. Important LiDAR metrics for discriminating forest tree species in Central Europe. ISPRS Journal of Photogrammetry and Remote Sensing. 137: 163-174. doi.org/10.1016/j.isprsjprs.2018.02.002.

Silva, C.A., Crookston, N.L., Hudak, A.T., and Vierling, L.A. 2015. rLiDAR: An R package for reading, processing and visualizing LiDAR (Light Detection and Ranging) data. Available from http://cran.rproject.org/web/packages/rLiDAR/index.html [accessed 15 January 2019].

Smits, I., Prieditis, G., Dagis, S., and Dubrovskis, D. 2012. Individual tree identification using different LIDAR and optical imagery data processing methods. Biosystems and Information Technology. 1: 19-24. doi.org/10.11592/bit.121103.

SoEF. (2020). Summary for Policy Markers State of Europe's Forest 2020. (Vol. 4, pp. 64–75).

Tabacchi, G., Di Cosmo, L., and Gasparini, P. 2011. Aboveground tree volume and phytomass prediction equations for forest species in Italy. Eur. J. For. Res. 130(6): 911-934. doi.org/10.1007/s10342-011-0481-9.

Torresan, C., Carotenuto, F., Chiavetta, U., Miglietta, F., Zaldei, A., and Gioli, B. 2020. Individual Tree Crown Segmentation in Two-Layered Dense Mixed Forests from UAV LiDAR Data. Drones. 4(2): 10. doi:10.3390/drones4020010.

Torresan, C., Benito Garzón, M., O'Grady, M., Robson, T.M., Picchi, G., Panzacchi P., Tomelleri, E., Smith, M., Marshall, J.D., Wingate, L., Tognetti, R. 2021. A new generation of sensors and monitoring tools to support climate-smart forestry practices. Canadian Journal of Forest Research, (ja). 1-47. Just-IN https://doi.org/10.1139/cjfr-2020-0295

Wang, Y., Hyyppä, J., Liang, X., Kaartinen, H., Yu, X., Lindberg, E., Holmgren, J., Qin, Y., Mallet, C., Ferraz, A., Torabzadeh, H., Morsdorf, F., Zhu, L., Liu, J., and Alho, P. 2016. International benchmarking of the individual tree detection methods for modeling 3-D canopy structure for silviculture and forest ecology using airborne laser scanning. IEEE Transactions on Geoscience and Remote Sensing. 54(9): 5011-5027. doi.org/10.1109/TGRS.2016.2543225.

Wang, Y., Pyörälä, J., Liang, X., Lehtomäki, M., Kukko, A., Yu, X., Kaartinen, H., and Hyyppä, J. 2019. In situ biomass estimation at tree and plot levels: What did data record and what did algorithms derive from terrestrial and aerial point clouds in boreal forest. Remote Sensing of Environment. 232:1-15. doi.org/10.1016/j.rse.2019.111309.

Wang, Y., Lehtomäki, M., Liang, X., Pyörälä, J., Kukko, A., Jaakkola, A., Liu, J., Feng, Z., Chen, R., and Hyyppä, J. 2019a. Is field-measured tree height as reliable as believed–A comparison study of tree height estimates from field measurement, airborne laser scanning and terrestrial laser scanning in a boreal forest. ISPRS journal of photogrammetry and remote sensing. 147: 132-145. https://doi.org/10.1016/j.isprsjprs.2018.11.008.

White, J.C., Wulder, M.A., and Buckmaster, G. 2014. Validating estimates of merchantable volume from airborne laser scanning (ALS) data using weight scale data. The Forestry Chronicle. 90(3): 378-385. doi.org/10.5558/tfc2014072.

Williams, J., Schönlieb, C.B., Swinfield, T., Lee, J., Cai, X., Qie, L., and Coomes, D.A. 2019. Three-dimensional Segmentation of Trees Through a Flexible Multi-Class Graph Cut Algorithm (MCGC). IEEE Trans. Geosci. Electron. 1-23. doi.org/10.1109/

TGRS.2019.2940146.

Yu, X., Hyyppä, J., Holopainen, M., and Vastaranta, M. 2010. Comparison of area-based and individual tree-based methods for predicting plot-level forest attributes. Remote Sens. 2(6): 1481-1495. doi.org/10.3390/rs2061481.

List of Table:

Absolute (m^3 and tons) and percent (%) values of bias and root means squared error (RMSE) were even displayed.

List of Figures:

Figure 1. Location of study area Bosco Pennataro (red triangle) and location of the field plots (ADS). This figure has been made using the Italian boundaries shapefile (https://www.istat.it/) through QGIS software, while Bosco Pennataro raster has been surveyed as part of the FREShLIFE project "Demonstrating Remote Sensing integration in sustainable forest management" (LIFE14/ IT000414).

Figure 2. Methodological workflow applied to derive the carbon stock at the single tree level, using Airborne Laser Scanning (ALS) data. The ALS data was cut using the field plots (ADS) box dimensions and stratified into lower (Layer1), intermediate (Layer2) and upper (Layer3) canopy layers. The root mean squared error (RMSE) and coefficient of determination (R-squared) values for tree volume prediction was even displayed.

Figure 3. Workflow of the processing of the Airborne Laser Scanning (ALS) point cloud for each canopy layer (Layer1, Layer2 and Layer3) within each field plot (ADS). The diameter at breast height (DBH) and tree height (TH) were considered in the categorization step.

Figure 4. The processing of the Airborne Laser Scanning (ALS) point cloud through Density-Based Spatial Clustering of Applications with Noise (DBSCAN) algorithm. The minimum number of points (MinPts) and the Eps neighborhood distance ($N_{Eps}(p)$) thresholds were considered.

Figure 5. Workflow of the processing for detecting the trees across the three canopy layers (i.e. lower layer: Layer1, intermediate layer: Layer2 and upper layer: Layer3) from Airborne Laser Scanning (ALS) point cloud. The minimum number of points (MinPts) and Eps neighborhood distance (Eps) thresholds were used for processing Density-Based Spatial Clustering of Applications with Noise (DBSCAN) and K-means.

Figure 6. Graphical distribution of the field plots (ADS) according to the average point density (APD; Points m^{-2}) and the standard deviation of tree height (TH_{sd}; m) for each category from A to D groups (A, highly difficult; B, moderately easy; C, highly easy; D, moderately difficult).

Figure 7. Four representative maps of the four different Airborne Laser Scanning (ALS) point cloud combinations (one per category). The red square showed the field plots (ADS) border; the number of trees (N°trees; units) was showed for every canopy layer (i.e. lower layer: Layer1, intermediate layer: Layer2 and upper layer: Layer3); the tree height (TH; m) and the diameter at breast height (DBH; cm) were expressed in average and the standard deviation (SD; ±) values; the top letters report the category level (i.e. A, highly difficult; B, moderately easy; C, highly easy; D, moderately difficult).

Figure 8. Comparison between predicted vs. observed values of I) detection rate (DR; %), II) Euclidean distance (m), III) tree crown overlap (%), and IV) time for tree detection (Time for TD; sec) for each canopy layer (Layer1 "L1", Layer2 "L2", and Layer3 "L3") and for every category (highly difficult, moderately easy, highly easy and moderately difficult). The average values of the time consuming for detecting tree (time for TD, sec) belonging to each study area was displayed for each category.

Figure 9. Predicted values vs. observed forest inventory variables. The box A) shows diameter at breast height (DBH, cm); box B) shows tree height (TH; m) and box C) displays stem volume (VOL, m^3). The number of trees (N°trees; units), number of predictors (N°predictors; units), coefficient of determination (R-squared; 0-1) and root mean squared error (RMSE; cm, m and m^3) were even reported.

Table 1. Summary of forest stand characteristics of Airborne Laser Scanning (ALS) and forest inventory data per each field plot (ADS) and complexity categories. The average point density (APD; Points m^{-2}), average point spacing (APS; m), diameter at breast height (DBH; cm) and tree height (TH; m) were estimated per ADS. The stem volume (VOL; m^{3}) and carbon stock (CS; tons) were estimated per hectare (Ha.). The number of trees (N°trees; units) were calculated per ADS and Ha. The mean (^{a}) and sum (^{b}) and standard deviation (^{c}) values were showed.

Category	ADS	**ALS data**		**Forest inventory data**					
		ADS					Ha		
		APD^{a} (Points m^{-2})	APS^{a} (m)	N°trees^{2} (units)	DBH^{a} (cm)	TH^{a} (m)	N°trees^{b} (units)	VOL^{b} (m^{3})	CS^{b} (ton)
Highly difficult	6	30	0.2	32	18	17.3	604	220.3	61.5
	8	13.8	0.3	52	15.7	13.7	981	307.8	86
	9	14.9	0.3	47	19	16.3	887	353.4	98.7
	11	30	0.2	86	15.2	12.9	1623	341.7	95.4
	15	16.3	0.3	196	9.9	8.2	3698	183	51.1
	16	23.4	0.2	121	12.1	9.4	2302	272.1	76
	18	16.8	0.2	95	12.9	9.7	1792	277.3	77.4
	21	30	0.2	101	14	11.4	1906	329	91.9
	(^{a})	*21.9*	*0.2*	*91*	*14.6*	*12.4*	*1724*	*285.6*	*79.8*
	(^{b})			***730***			*13792*		
	(^{c})	*7.3*	*0.1*	*52*	*3*	*3.3*	*985*	*60*	*16.8*
Moderately easy	5	17.2	0.2	34	20	18.2	642	325.9	91
	13	26.5	0.2	83	16.5	14.6	1566	488.3	136.4
	17	12.1	0.3	58	18.1	13.3	1094	485.9	135.7
	20	20.8	0.2	31	21.1	16	585	308.8	86.3
	22	13.9	0.3	70	17.1	15.6	1321	633.9	177
	24	13.5	0.3	42	18.6	16.2	792	406.4	113.5
	27	31	0.2	54	13.5	11.1	1019	408.1	114
	31	23	0.2	63	17.1	14	1189	435.2	121.5
	(^{a})	*19.75*	*0.24*	*54*	*17.75*	*14.88*	*1026*	*436.56*	*121.93*
	(^{b})			***435***			*8208*		
	(^{c})	*6.78*	*0.05*	*18*	*2.32*	*2.14*	*339*	*103.06*	*28.77*
Highly easy	4	62.5	0.1	49	17.8	15.3	925	357.2	99.8
	7	74.4	0.1	36	20	13.3	679	450.2	125.7
	10	73.7	0.1	37	23.1	16.9	698	528.5	147.6
	25	81.6	0.1	32	20.7	21.3	623	430.4	120.2
	26	48.6	0.1	24	25.8	23.1	453	477.1	133.3
	29	292.9	0.1	60	16.1	15.4	1132	400	111.7
	30	68.7	0.1	60	16.5	13.9	1132	413.6	115.5
	(^{a})	*100.3*	*0.1*	*43*	*20*	*17*	*806*	*436.7*	*122*
	(^{b})			***298***			*5642*		
	(^{c})	*85.6*	*0*	*14*	*3.6*	*3.8*	*262*	*55.5*	*15.5*
Moderately difficult	1	31.3	0.2	33	20.5	18.5	623	249	69.6
	2	227.6	0.1	120	12.8	9.8	2264	270.8	75.6
	3	96.6	0.1	35	26.9	17.1	660	537.5	150.1
	12	67.1	0.1	140	10.6	9.1	2642	286.8	80.1
	14	99.9	0.1	91	11.6	9.8	1717	344.7	96.3

19	84.3	0.1	50	20.1	14.3	943	295.4	82.5
23	43.8	0.2	53	18	12.3	1000	390.7	109.1
28	202.7	0.1	132	10.7	10.8	2491	220.2	61.5
([a])	*106.66*	*0.13*	*82*	*16.4*	*12.71*	*1542*	*324.39*	*90.6*
([b])			***654***			*12340*		
([c])	*71.41*	*0.05*	*45*	*5.92*	*3.57*	*840*	*101.34*	*28.29*

Table 2. Tree detection results. Number of stems observed from reference data (TR; units) and number of stems predicted from ALS data (T_{ALS}; units), true positive (TruePos; units), false positive (FalsePos; units), false negative (FalseNeg; units) and detection rate (DR; %) for lower (Layer1), intermediate (layer2) and upper (Layer3) canopy layers.

Tree detection results								
Categories	**Canopy layers**	**TR (units)**	**T_{ALS} (units)**	**Tree detection TruePos (units)**	**FalsePos (units)**	**FalseNeg (units)**	**DR (%)**	
Highly difficult	Layer1	245	124	69	55	176	28	
	Layer2	237	176	101	75	136	43	
	Layer3	248	147	91	56	157	37	
	Sum	**730**	447	**261**	186	469		
	Mean & SD (±)						***36***	***(±7.3)***
Moderately easy	Layer1	144	54	40	14	104	28	
	Layer2	141	120	78	42	63	55	
	Layer3	150	147	97	50	53	65	
	Sum	**435**	321	**215**	106	220		
	Mean & SD (±)						***49***	***(±19.2)***
Highly easy	Layer1	99	178	63	115	36	64	
	Layer2	96	213	70	143	26	73	
	Layer3	103	170	61	109	42	59	
	Sum	**298**	561	**194**	367	104		
	Mean & SD (±)						***65***	***(±7.0)***
Moderately difficult	Layer1	218	166	108	58	110	50	
	Layer2	213	147	97	50	116	46	
	Layer3	223	105	77	28	146	35	
	Sum	**654**	418	**282**	136	372		
	Mean & SD (±)						***43***	***(±7.8)***
Layer1	*Sum*	706	522	280	242	426		
	Mean & SD (±)						***42***	***(±17.5)***
Layer2	*Sum*	687	656	346	310	341		
	Mean & SD (±)						***54***	***(±13.7)***
Layer3	*Sum*	724	569	326	243	398		
	Mean & SD (±)						***49***	***(±15.4)***
Total	*Sum*	2117	1747	952	795	1165		
	Mean & SD (±)						***48***	***(±12.5)***

Table 3. Summary statistics of the forest inventory variables estimated with the Random Forests algorithm by using top-nine metrics for diameter at breast height (DBH; cm), tree height (TH; m), and stem volume (VOL; m^3). The number of trees (N°trees; units), coefficient of determination (R-squared; 0-1) and root mean squared error (RMSE; cm, m and m^3) were displayed. The outcomes were displayed for all four categories (highly difficult, moderately easy, highly easy and moderately difficult), which was further divided by lower (Layer1), intermediate (Layer2) and upper (Layer3) canopy layers.

Category	Statistic measurements	**Linear regression** DBH (cm)				TH (m)				VOL (m^3)			
		Layer1	Layer2	Layer3	Layer1 - Layer3	Layer1	Layer2	Layer3	Layer1 - Layer3	Layer1	Layer2	Layer3	Layer1 - Layer3
Highly difficult	N°trees	69	101	91	**261**	69	101	91	**261**	69	101	91	**261**
	R-squared	0.91	0.91	0.89	0.9	0.92	0.91	0.91	0.95	0.93	0.87	0.91	0.9
	RMSE	0.9	2.25	3.8	3.62	1.05	1.01	1.03	1.14	0.01	0.05	0.27	0.2
Moderately easy	N°trees	40	78	97	**215**	40	78	97	**215**	40	78	97	**215**
	R-squared	0.91	0.89	0.88	0.9	0.92	0.92	0.89	0.93	0.78	0.89	0.87	0.89
	RMSE	1.44	2.43	4.25	4.59	0.7	0.93	1.1	1.38	0.02	0.08	0.37	0.35
Highly easy	N°trees	63	70	61	**194**	63	70	61	**194**	63	70	61	**194**
	R-squared	0.82	0.89	0.91	0.91	0.82	0.93	0.9	0.95	0.8	0.89	0.88	0.9
	RMSE	1.77	3.26	4.28	4.63	1.87	1.07	1.25	1.56	0.04	0.12	0.56	0.4
Moderately difficult	N°trees	108	97	77	**282**	108	97	77	**282**	108	97	77	**282**
	R-squared	0.88	0.9	0.89	0.91	0.86	0.97	0.89	0.95	0.81	0.86	0.91	0.9
	RMSE	1.38	3.3	5.15	4.08	1.16	0.61	1.52	1.21	0.02	0.15	0.38	0.24

Table 4. Comparison between predicted and observed values of stem volume (VOL; m^3) and carbon stock (CS; tons) derived from Airborne Laser Scanning (ALS) metrics. These values were furtherly displayed by each category (highly difficult, moderately easy, highly easy and moderately difficult) and by each field plot (ADS). The number of trees (N°trees; units) was calculated per ADS and ha^{-1}. Absolute (m^3 and tons) and percent (%) values of bias and root means squared error (RMSE) were even displayed.

Stem volume and carbon stock prediction											
		N°trees		VOL (m^3 ha^{-1})		CS (tons ha^{-1})		VOL	CS	VOL and CS	
Category	ID	ADS	Ha^{-1}	Observed	Predicted	Observed	Predicted	Bias (m3 ha-1)	Bias (tons.ha-1)	Bias (%)	RMSE (%)
Highly difficult	6	29	547	185.5	227	51.8	63.4				
	8	22	415	253	245.2	70.7	68.5				
	9	34	641	304.1	305.1	84.9	85.2				
	11	28	528	143.5	146.9	40.1	41				
	15	40	755	34.2	32.4	9.6	9.1				
	16	40	755	105.1	102.6	29.4	28.7				
	18	31	585	119.8	131.8	33.5	36.8				
	21	37	698	175.1	148.9	48.9	41.6				
	Sum	*261*	*4924*								
	Mean			*165*	*167.5*	*46.1*	*46.8*				
	Accuracy							*-2.4*	*-0.7*	*1.5*	*1.48*
Moderately easy	5	30	566	322	325.2	89.9	90.8				
	13	38	717	277.2	310.8	77.4	86.8				
	17	20	377	306.2	284.1	85.5	79.3				
	20	17	321	200.1	212.3	55.9	59.3				
	22	43	811	471.7	493.3	131.7	137.8				
	24	19	358	304	308.4	84.9	86.1				
	27	16	302	256.4	227.5	71.6	63.5				
	31	32	604	338.9	318.3	94.7	88.9				
	Sum	*215*	*4056*								
	Mean			*309.6*	*310*	*86.5*	*86.6*				
	Accuracy							*-0.4*	*-0.1*	*0.1*	*0.14*
Highly easy	4	34	641	192.4	198.7	53.7	55.5				
	7	20	377	417.1	324	116.5	90.5				
	10	28	528	388.7	372.2	108.6	104				
	25	23	434	392.3	420.6	109.6	117.5				
	26	21	396	441.6	462.3	123.3	129.1				
	29	44	830	304.3	371.1	85	103.7				
	30	24	453	158.4	164.6	44.2	46				
	Sum	*194*	*3659*								
	Mean			*327.8*	*330.5*	*91.6*	*92.3*				
	Accuracy							*-2.7*	*-0.8*	*0.8*	*0.83*
M	1	22	415	172.7	188.2	48.2	52.6				

	2	40	755	29.7	44.3	8.3	12.4				
	3	25	472	406.5	407.6	113.6	113.8				
	12	32	604	68.5	58	19.1	16.2				
	14	25	472	170.6	177.9	47.7	49.7				
	19	41	774	265.5	253.9	74.2	70.9				
	23	22	415	159.7	147.6	44.6	41.2				
	28	75	1415	119.8	111.4	33.5	31.1				
	Sum	*282*	*5322*								
	Mean			*174.1*	*173.6*	*48.6*	*48.5*				
ode rat	*Accuracy*							*0.5*	*0.1*	*-0.3*	*0.3*

Draft

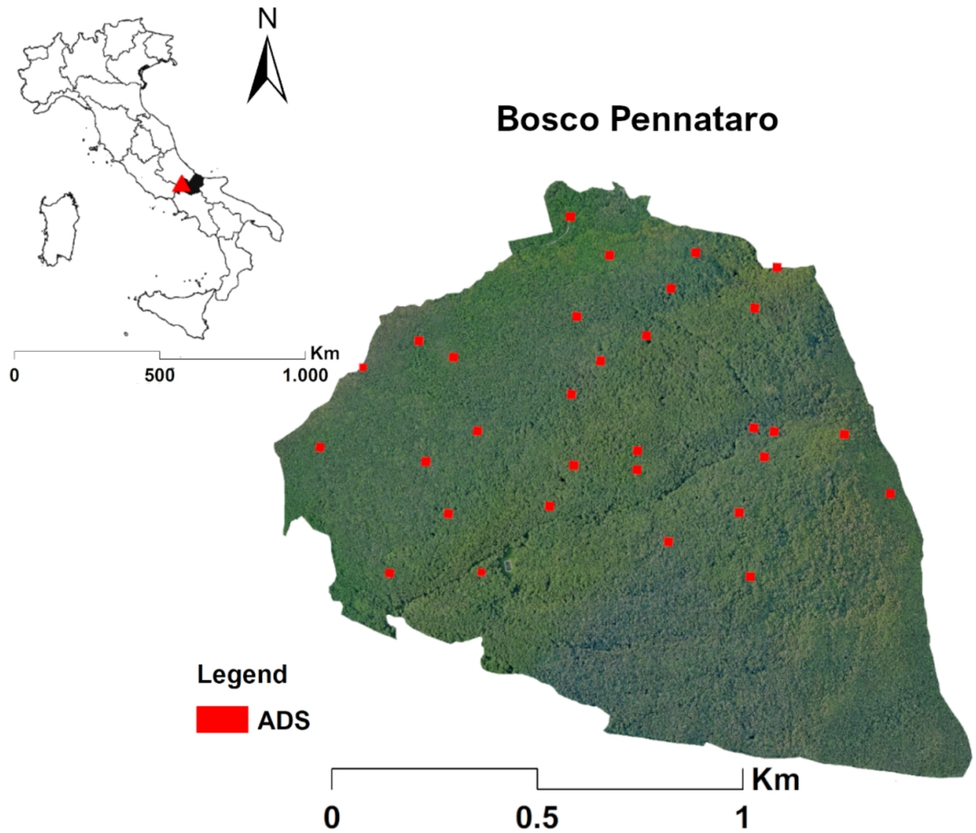

Figure 1. Location of study area Bosco Pennataro (red triangle) and location of the field plots (ADS). This figure has been made using the Italian boundaries shapefile (https://www.istat.it/) through QGIS software, while Bosco Pennataro raster has been surveyed as part of the FREShLIFE project "Demonstrating Remote Sensing integration in sustainable forest management" (LIFE14/ IT000414).

119x99mm (300 x 300 DPI)

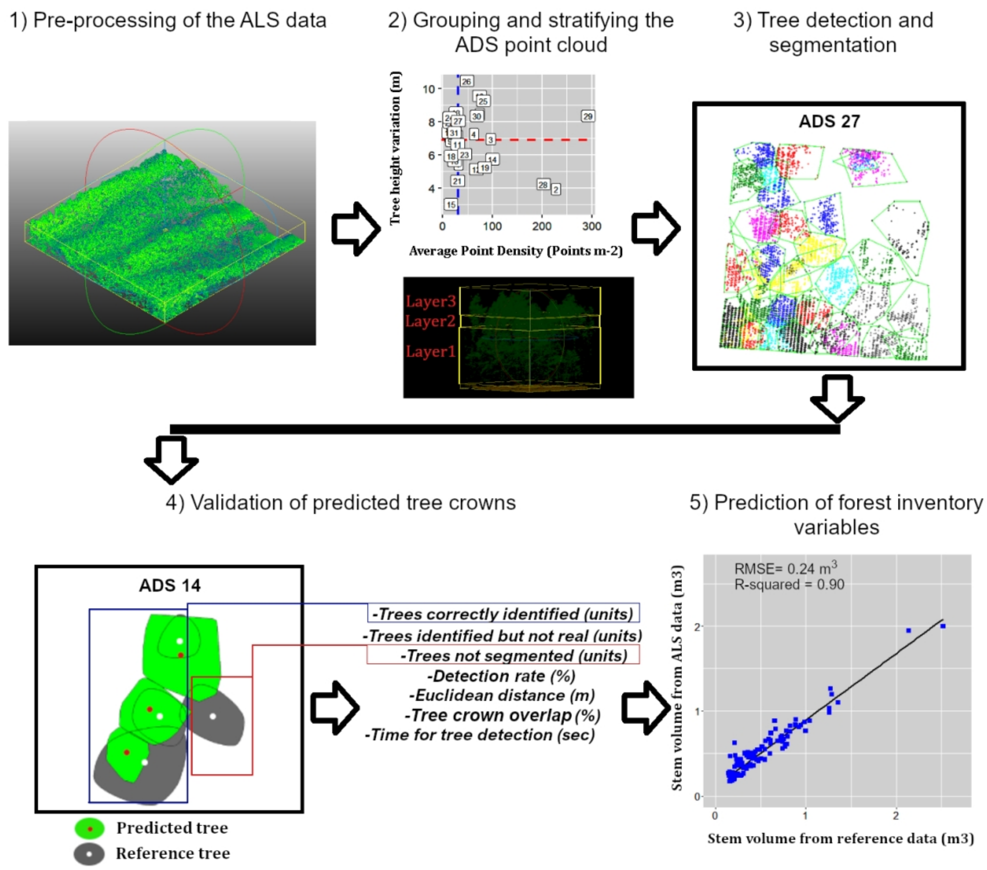

Figure 2. Methodological workflow applied to derive the carbon stock at the single tree level, using Airborne Laser Scanning (ALS) data. The ALS data was cut using the field plots (ADS) box dimensions and stratified into lower (Layer1), intermediate (Layer2) and upper (Layer3) canopy layers. The root mean squared error (RMSE) and coefficient of determination (R-squared) values for tree volume prediction was even displayed.

119x105mm (300 x 300 DPI)

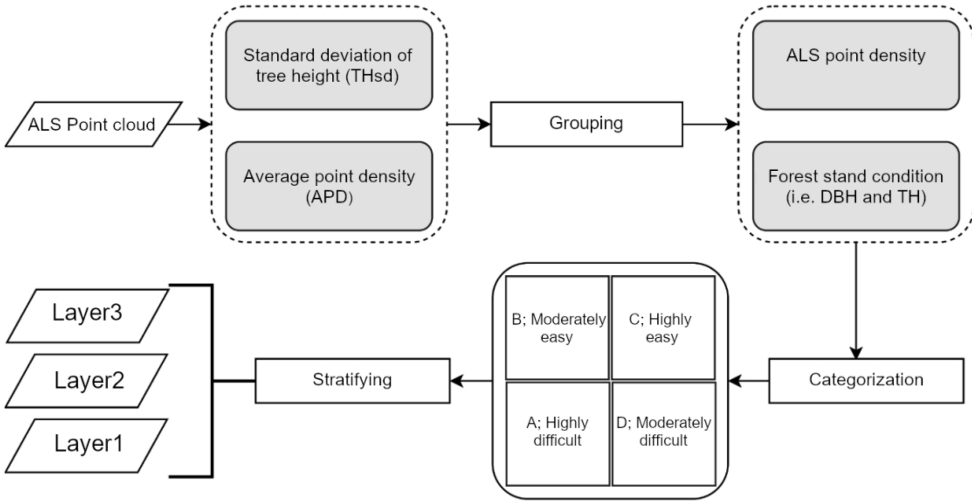

Figure 3. Workflow of the processing of the Airborne Laser Scanning (ALS) point cloud for each canopy layer (Layer1, Layer2 and Layer3) within each field plot (ADS). The diameter at breast height (DBH) and tree height (TH) were considered in the categorization step.

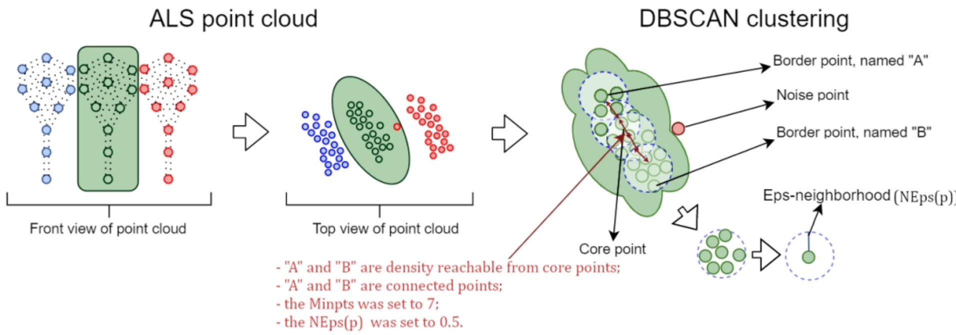

Figure 4. The processing of the Airborne Laser Scanning (ALS) point cloud through Density-Based Spatial Clustering of Applications with Noise (DBSCAN) algorithm. The minimum number of points (MinPts) and the Eps neighborhood distance (NEps(p)) thresholds were considered.

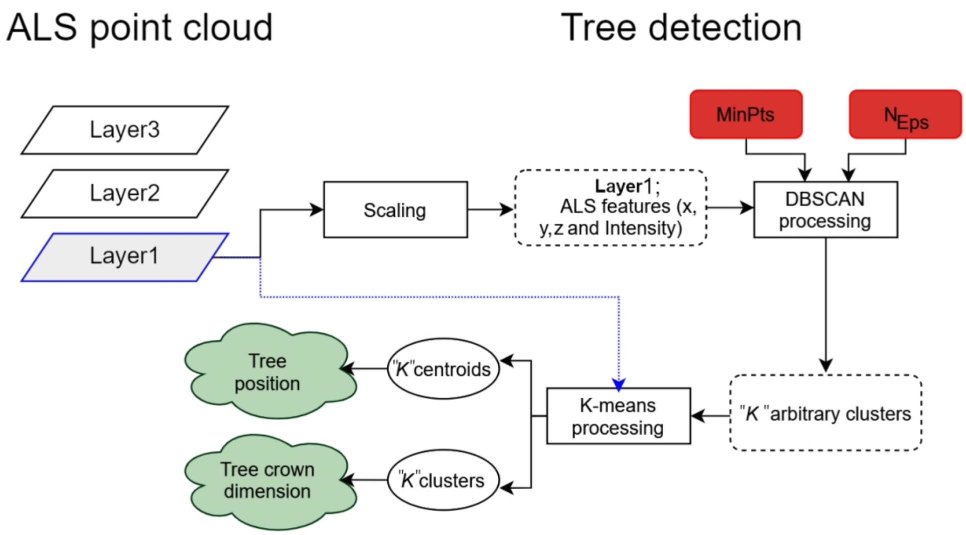

Figure 5. Workflow of the processing for detecting the trees across the three canopy layers (i.e. lower layer: Layer1, intermediate layer: Layer2 and upper layer: Layer3) from Airborne Laser Scanning (ALS) point cloud. The minimum number of points (MinPts) and Eps neighborhood distance (Eps) thresholds were used for processing Density-Based Spatial Clustering of Applications with Noise (DBSCAN) and K-means.

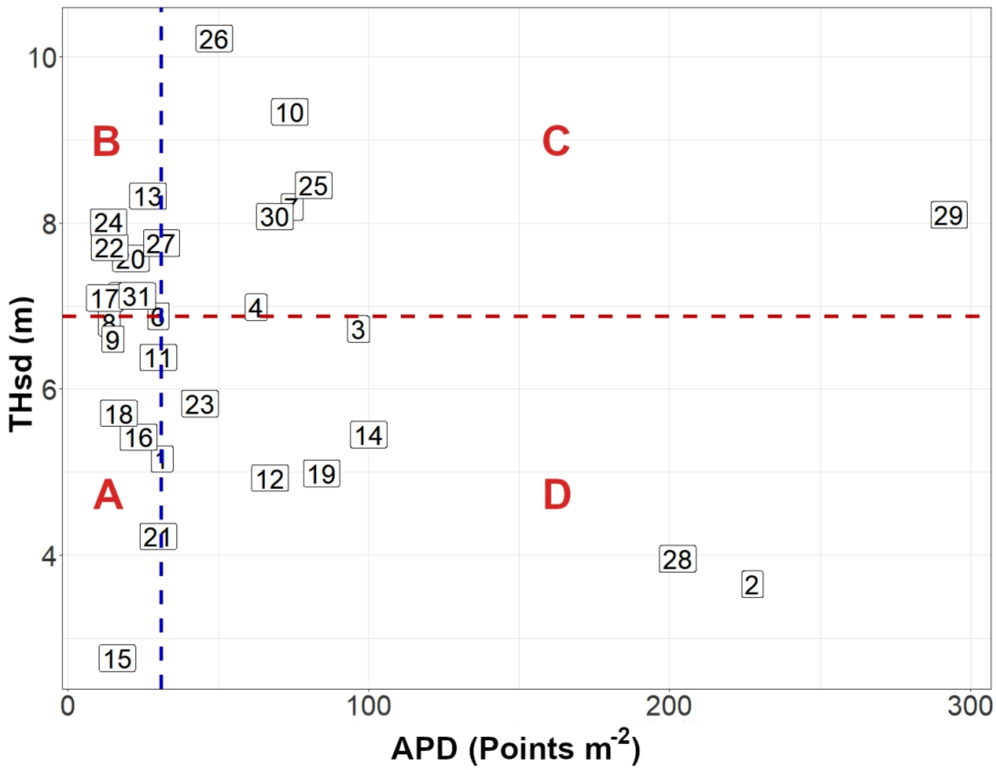

Figure 6. Graphical distribution of the field plots (ADS) according to the average point density (APD; Points m-2) and the standard deviation of tree height (THsd; m) for each category from A to D groups (A, highly difficult; B, moderately easy; C, highly easy; D, moderately difficult).

119x99mm (300 x 300 DPI)

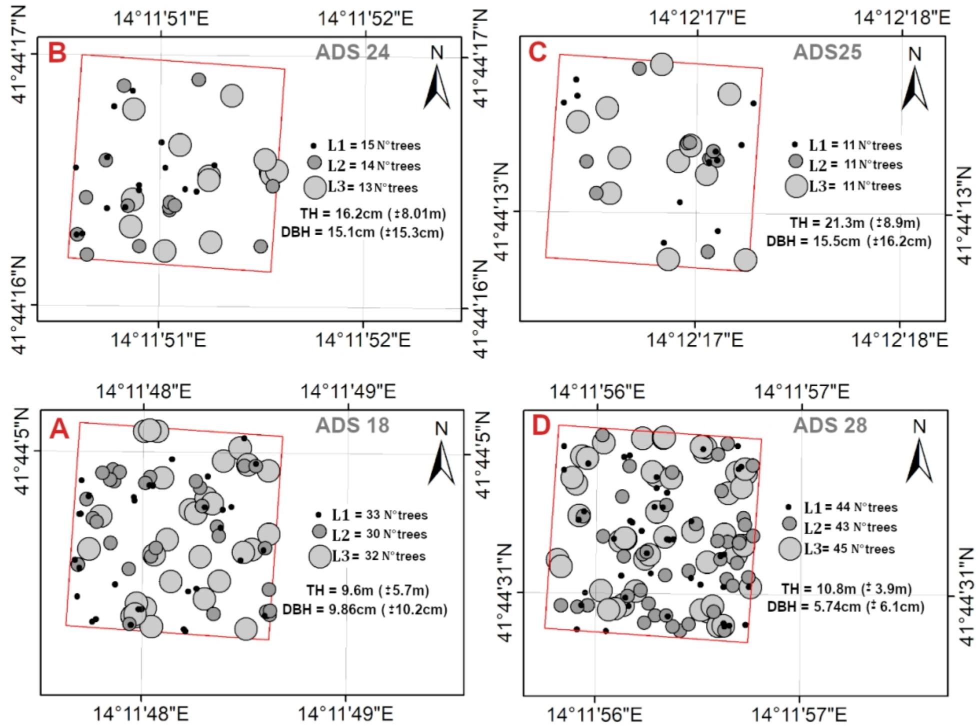

Figure 7. Four representative maps of the four different Airborne Laser Scanning (ALS) point cloud combinations (one per category). The red square showed the field plots (ADS) border; the number of trees (N°trees; units) was showed for every canopy layer (i.e. lower layer: Layer1, intermediate layer: Layer2 and upper layer: Layer3); the tree height (TH; m) and the diameter at breast height (DBH; cm) were expressed in average and the standard deviation (SD; ±) values; the top letters report the category level (i.e. A, highly difficult; B, moderately easy; C, highly easy; D, moderately difficult).

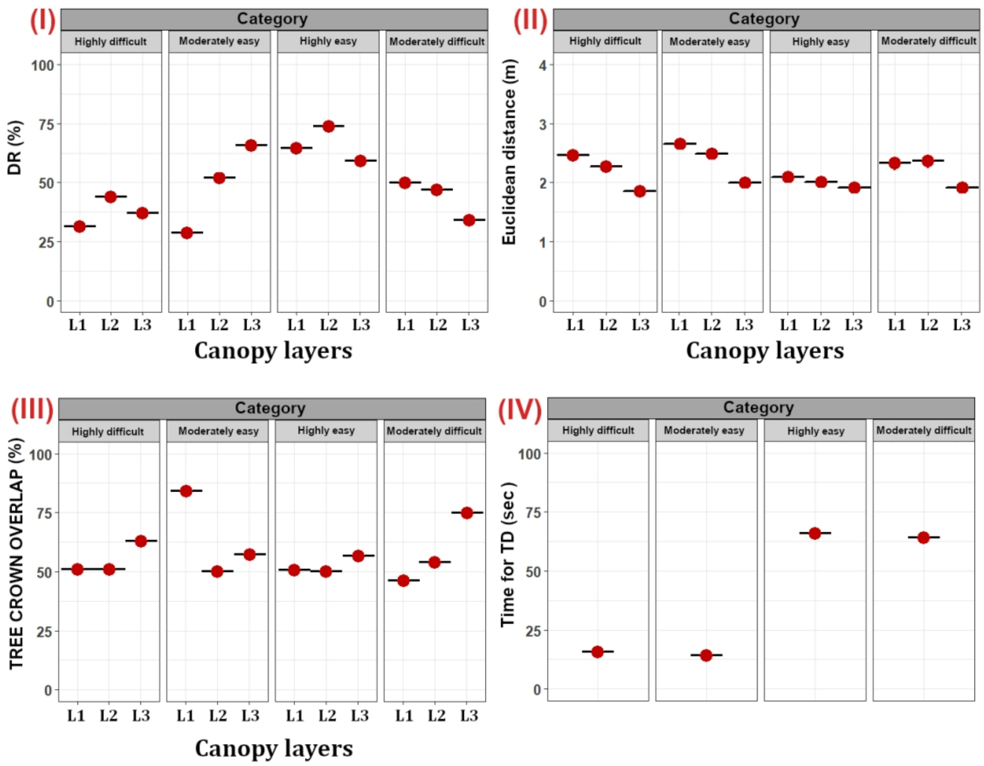

Figure 8. Comparison between predicted vs. observed values of I) detection rate (DR; %), II) Euclidean distance (m), III) tree crown overlap (%), and IV) time for tree detection (Time for TD; sec) for each canopy layer (Layer1 “L1”, Layer2 “L2”, and Layer3 “L3”) and for every category (highly difficult, moderately easy, highly easy and moderately difficult). The average values of the time consuming for detecting tree (time for TD, sec) belonging to each study area was displayed for each category.

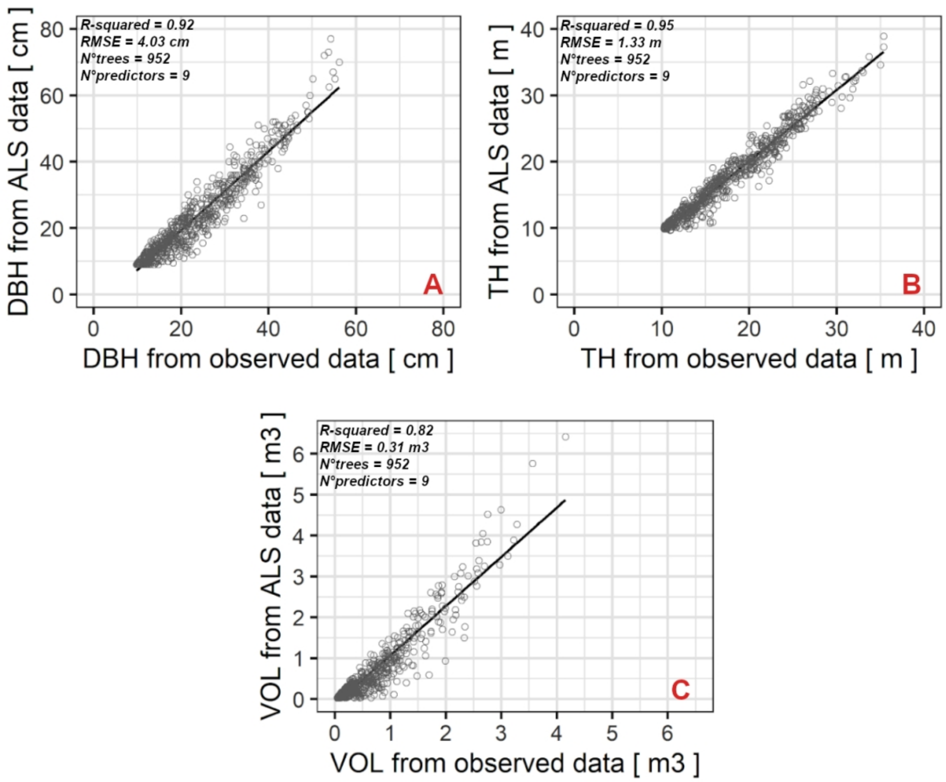

Figure 9. Predicted values vs. observed forest inventory variables. The box A) shows diameter at breast height (DBH, cm); box B) shows tree height (TH; m) and box C) displays stem volume (VOL, m^3). The number of trees (N°trees; units), number of predictors (N°predictors; units), coefficient of determination (R-squared; 0-1) and root mean squared error (RMSE; cm, m and m3) were even reported.

119x97mm (300 x 300 DPI)